Liquid Crystals
Publication details, including instructions for authors and subscription information:
http://www.informaworld.com/smpp/title~content=t713926090

A phenomenological model for the undulating twist grain boundary-C* phase

P. A. Pramod; Yashodhan Hatwalne; N. V. Madhusudana

Online publication date: 06 August 2010

To cite this Article Pramod, P. A. , Hatwalne, Yashodhan and Madhusudana, N. V.(2001) 'A phenomenological model for the undulating twist grain boundary-C* phase', Liquid Crystals, 28: 4, 525 — 533
To link to this Article: DOI: 10.1080/02678290010018033
URL: http://dx.doi.org/10.1080/02678290010018033

LIQUID CRYSTALS, 2001, VOL. 28, NO. 4, 525–533

A phenomenological model for the undulating twist grain boundary-C* phase

P. A. PRAMOD†, YASHODHAN HATWALNE and N. V. MADHUSUDANA*
Raman Research Institute, Bangalore 560 080, India

(*Received 2 August 2000; accepted 24 August 2000*)

We propose a simple phenomenological model which is able to account for the various twist grain boundary (TGB) phases, including the recently discovered undulating twist grain boundary-C* ($UTGB_{C^*}$) phase. In the $UTGB_{C^*}$ phase, the smectic C* (SmC*)-like blocks and the grain boundaries separating them undulate to form a two-dimensional square lattice perpendicular to the TGB helix axis. We treat the grain boundaries separating adjacent smectic blocks as interfaces with an anisotropic interfacial tension. At moderate chiral strengths we find a TGB_A–TGB_C–SmC* sequence. As the chiral strength is increased this goes to the sequence TGB_A–$UTGB_{C^*}$–SmC*. Such sequences have been observed experimentally.

1. Introduction

The analogy between the nematic–smectic A transition in liquid crystals and the normal metal–superconductor transition was established by de Gennes [1, 2]. Renn and Lubensky exploited this analogy to predict the twist grain boundary (TGB) phase of liquid crystals made of chiral molecules [3, 4]. The TGB phase is to smectic liquid crystals as the Abrikosov flux lattice phase [5, 6] is to type-II superconductors. In a smectic A (SmA) phase the molecular (Frank) director plays the role of the vector potential for a special class of gauge transformations which satisfy $\hat{\mathbf{n}} \rightarrow \hat{\mathbf{n}} + \nabla\chi$, with $\nabla^2\chi = 0$, and the strength of chiral interaction is like the external magnetic field in the case of superconductors. Screw dislocations in SmA are like flux tubes in superconductors. However, in contrast to the triangular Abrikosov flux lattice, the screw dislocations in the TGB_A phase are arranged as a regular helical array of twist grain boundaries, as represented in figure 1. Independently of the theoretical prediction, Goodby *et al.* discovered such a phase [7]. Subsequent freeze fracture experiments confirmed the presence of arrays of screw dislocations in the TGB_A structure [8].

The detailed theoretical analysis of Renn and Lubensky [3], which led to the prediction of the TGB_A phase, closely follows that of Abrikosov for type-II superconductors. Type-II SmA is transformed to the TGB_A phase if the strength of chiral interaction exceeds a critical value (the lower critical field) at which the chiral energy gain from the twist overcomes the energy cost of creating screw dislocations. The upper critical chiral strength is given by the limit of stability of the cholesteric phase (the liquid crystal analogue of a normal metal in an external magnetic field) to the formation of the TGB_A phase. Benguigui [9] has very recently shown that near the weakly first order SmA–cholesteric transition, the interfacial tension between these phases can become negative for a sufficiently large Ginzburg parameter (the ratio of twist penetration depth to the correlation length), i.e. for type-II materials. This should favour the formation of screw dislocations near the transition temperature.

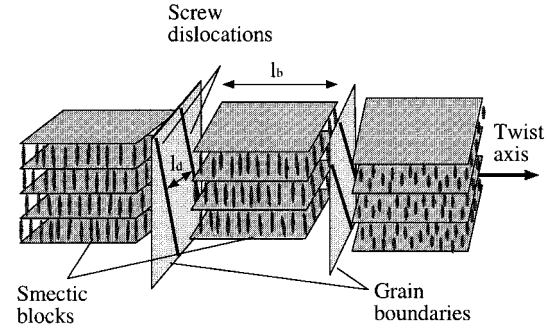

Figure 1. A schematic diagram of the TGB_A structure. The pitch of the structure is determined by the distance l_d between the screw dislocations within a grain boundary, the distance l_b between grain boundaries and the smectic layer spacing d. In TGB_A, l_d and l_b are typically of the order of a few hundred angstroms.

The rich variety of layered smectic phases has motivated the experimental search for and theoretical analysis of new types of TGB phases. Renn and Lubensky [10] also predicted a TGB_C phase in which the layer normals of the smectic C (SmC)-like blocks are parallel to the planes of the twist grain boundaries. In the TGB_C phase discovered by the Bordeaux group [11] the layer

*Author for correspondence; e-mail: nvmadhu@rri.ernet.in
†Present address: Laboratoire Physicochimie Curie, Institut Curie, F-75231 Paris Cedex 05, France.

Liquid Crystals ISSN 0267-8292 print/ISSN 1366-5855 online © 2001 Taylor & Francis Ltd
http://www.tandf.co.uk/journals
DOI: 10.1080/02678290010018033

normals of the successive SmC-like blocks rotate on a cone about the helix axis. This phase has a helielectric structure which is different from that of the theoretically anticipated ferroelectric TGB_C phase. Dozov has proposed a melted grain boundary (MGB) model for the Bordeaux TGB_C [12]. Whereas in the dislocation grain boundary model the molten regions are confined to the cores of the dislocations, in the MGB model the order parameter vanishes on entire surfaces. We however note the following: (i) screw dislocations have been seen in freeze fracture experiments in the TGB_A phase [8], and (ii) though in the first compound studied the TGB_C phase forms directly from the isotropic phase, later studies on other compounds have shown that the Bordeaux TGB_C phase also forms from the TGB_A phase on cooling [11]. We also point out that using a covariant elasticity theory for type-II SmC, Hatwalne and Lubensky [13] have shown that the lowest energy dislocations are not pure screw dislocations. The mixed dislocations which are tilted with respect to the layer normal favour the Bordeaux TGB_C structure.

On theoretical grounds Renn [14] predicted a TGB_{C*} phase in which heliscrew dislocations corresponding to the pitch of the SmC* liquid crystal produce a superstructure over and above that of the TGB helix produced by screw dislocations in the SmC* layer structure. In our view such a structure has not yet been found experimentally.

Recently a three-dimensionally modulated TGB phase was experimentally observed in a binary mixture of mesogenic compounds in this laboratory [15]. Based on various experimental observations the structure schematically shown in figure 2 was proposed for this liquid crystal. Calorimetric experiments have shown that this phase is thermodynamically stable [16]. The main structural features of this undulating twist grain boundary-C* ($UTGB_{C*}$) phase are as follows: (a) the smectic blocks have a SmC*-like local order, and (b) the grain boundaries separating adjacent blocks as well as the blocks themselves have periodic undulations in the form of a square lattice—all the grain boundaries and the blocks undulate along two orthogonal directions normal to the TGB helix axis (figure 3). Recently, Kuczynski and Stegemeyer [17] have also seen a modulated TGB structure in a binary mixture. They attribute this to the TGB_{C*} structure proposed by Renn. We feel that their observation of the square grid indicates that the structure corresponds to that of the $UTGB_{C*}$ phase. A comprehensive review of the various TGB phases has been given by Goodby [18].

More recently, some single component systems exhibiting square grid textures have been discovered [19, 20]. In the compound studied in [20], X-ray diffraction experiments show that in the TGB_A phase the ω-scans produce a Gaussian profile with a characteristic width of about 6.6°, whereas in the modulated TGB phase this width is about four times larger. Based on this observation the authors conclude that the smectic layer normals within the blocks are not strictly orthogonal to the helix axis of the modulated TGB phase. Further, the lattice spacing of the square grid remains constant with temperature, unlike in the $UTGB_{C*}$ phase reported in [15], in which the spacing shows a diverging behaviour very close to the $UTGB_{C*}$–TGB_A transition. From our experiments [15] we cannot determine whether the smectic layering in the $UTGB_{C*}$ phase is distorted.

In this paper we propose a simple model for the $UTGB_{C*}$ phase in which we treat the grain boundaries as interfaces with anisotropic interfacial energy. We show

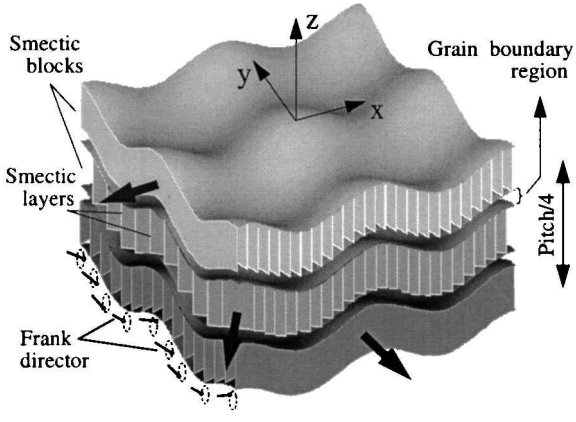

Figure 2. A schematic representation of the proposed structure for the $UTGB_{C*}$ phase. The two-dimensionally undulated grain boundary regions are shown. The smectic layer normals (large arrows) rotate from block to block. Within each block the Frank-director precesses along the layer normal direction as represented by the nails for the lowermost block.

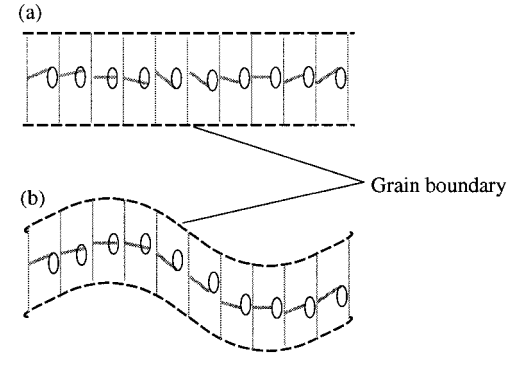

Figure 3. A schematic representation of (*a*) a smectic C* block with parallel interfaces, and (*b*) a smectic C* block with undulating interfaces. In (*a*) the director makes various angles with the interface whereas in (*b*) the director is everwhere parallel to the local tangent plane to the interface.

that this model reproduces experimentally observed phase sequences. Our principal results are summarized in the phase diagrams shown in figures 4 and 5. In what follows we discuss the basic physical motivation behind our model.

2. The interface model

Even for the TGB_A and TGB_C phases a first principles defect-lattice analysis which gives all the structural details (like the dislocation spacing within a grain boundary and the distance between grain boundaries) is not yet available. For the $UTGB_{C*}$ phase and related phase transitions such an analysis is clearly very complicated. We therefore content ourselves with a simplified phenomenological theory which we believe captures most of the essential physical features of the problem. Our main aim is to show that it is possible to have an equilibrium TGB structure having SmC*-like blocks separated by undulating grain boundaries.

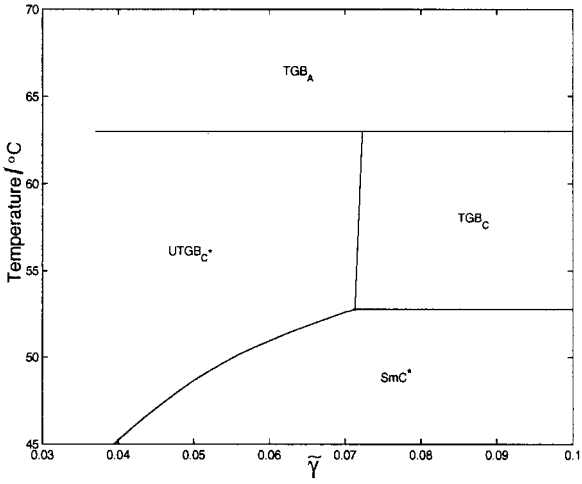

Figure 4. The T–$\tilde{\gamma}$ phase diagram showing the stability regions of the various phases for $\Lambda = 0.039$. Note that the line separating the $UTGB_{C*}$ and the TGB_C phases has a positive slope.

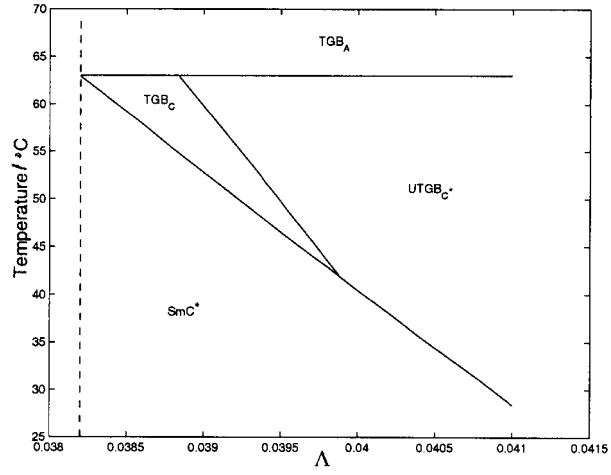

Figure 5. The T–Λ phase diagram showing the stability regions of the various phases with $\tilde{\gamma} = 0.072$. The vertical dashed line corresponds to the lower critical field $\Lambda_o = \sqrt{K\gamma}$. Below Λ_o the TGB phases are unstable.

Small angle grain boundaries in smectic liquid crystals are arrays of dislocations. Far away from the grain boundary the smectic layering is undistorted. Detailed line shape analysis of the quasi-Bragg X-ray diffraction spots corresponding to the TGB_A and TGB_C phases [21, 11] indicates that the smectic order within the blocks is well preserved. On the other hand, the smectic order within the grain boundaries is relatively weak due to the presence of screw dislocation arrays and the resultant twist deformation across them. It therefore appears reasonable to coarse-grain the dislocated structure of the grain boundary and treat it as an interface for studying the bulk properties of the TGB phases. It is also natural to expect that the 'interfacial tension' (grain boundary energy per unit area) is anisotropic, as in smectic–nematic and smectic–isotropic interfaces [22, 23].

We study the relative stability of the TGB phases and the SmC* phase as a function of temperature, the anisotropic interfacial tension and the chiral strength. For the sake of simplicity, we keep the size of the smectic-like blocks and the grain boundary angle in the TGB phases fixed. Experimentally it is known that the TGB_A and the TGB_C phases can be commensurate [24, 11]. It is not clear whether the $UTGB_{C*}$ phase is commensurate or not. In the proposed structure of the $UTGB_{C*}$ phase (see figure 2) each block is characterized by (i) a pair of orthogonal wave vectors of equal magnitude $(q_u\hat{\mathbf{x}}, q_u\hat{\mathbf{y}})$ corresponding to the undulation (this pair is the same for all the blocks), and (ii) a wavevector q_m of the helical pitch which is along the layer normal of the mth block. The angle β_m between q_m and the X-axis has an important structural significance. If $\tan\beta_m$ is irrational, one cannot define a unit cell for the structure in the mth block. We disregard this possibility and simplify our calculations further by assuming that the twist angle across the grain boundaries in the $UTGB_{C*}$ phase is $\pi/4$ (see figure 2), even though the measured values of this angle in the TGB_A and the TGB_C phases are smaller [24, 11]. We believe that this simplifying assumption does not make a qualitative difference in our phase diagram. With these assumptions we calculate the free energy for the $UTGB_{C*}$ structure by making an ansatz for the blocks and the grain boundary regions.

For small chiral strength and small tilt angles, we expect a transition from the TGB_A phase to the TGB_C phase, provided the interfacial tension is large enough. This is reminiscent of surface stabilized ferroelectric liquid crystal systems [25] in which the SmC* helix gets

unwound because of strong surface anchoring. For larger values of the chiral strength and for a given temperature (and hence tilt angle), we expect a transition from the TGB_C phase to the $UTGB_{C*}$ phase. This is because the chiral energy that can be gained in the bulk by having SmC*-like blocks overcomes the price to be paid at the interfaces. In the $UTGB_{C*}$ phase the interfaces are modulated for reasons described below.

Chiral interactions favour a twist deformation in the Frank-director. This tendency is expressed by the term linear in ($\mathbf{n} \cdot \nabla \times \mathbf{n}$) in the Frank free energy expression [1, 4]. The director distortion is a pure twist if the director is confined to a set of parallel planes orthogonal to the twist axis, as in the cholesteric phase. This is the case in TGB_A and TGB_C structures, where planes containing the director are always parallel to the grain boundaries. However, if the director configuration is close to that of SmC*, as in $UTGB_{C*}$, then a flat grain boundary is not the best way of maximizing the twist deformation across it. For simplicity, let us consider a single SmC* block bounded by grain boundaries on both sides. If the grain boundaries are flat the molecular tilt directions in different smectic layers make varying angles with respect to the grain boundaries as shown in figure 3(*a*), which is not energetically favoured in view of the anisotropic interfacial tension. Further, the distortion across the grain boundaries can no longer have the character of a pure twist. On the other hand, if the grain boundaries are allowed to undulate with the same periodicity as the SmC* structure, the director can be parallel to the local tangent plane of the grain boundary at all points as shown in figure 3(*b*). This increases the value of ($\mathbf{n} \cdot \nabla \times \mathbf{n}$) in the grain boundary region, thus lowering the net free energy. In our model this preference for the interface to lie parallel to the local director is taken into account via an anisotropic interfacial tension discussed below. Experimental observations suggest that the grain boundaries have a *two-dimensional* modulation with mutually orthogonal wave vectors. Also, all the grain boundaries undulate along the same two directions. But the smectic layer normal rotates from block to block. Therefore, in general, the director configuration is different in neighbouring blocks. Even so, the analysis presented here in which the grain boundaries are assumed to be interfaces with an anisotropic interfacial energy shows that the grain boundary energy is lower for an undulating grain boundary compared with that for a flat one. The modelling of the grain boundaries and smectic blocks is described below.

In the TGB_A and the TGB_C phases the grain boundaries are flat and are orthogonal to the TGB helix axis. In the former the twist deformation decays exponentially on going away from the grain boundaries [26]; the grain boundary regions are highly distorted. If l_d is the separation between screw dislocations within a TGB_A grain boundary and ε the energy per unit length of the dislocation, the dislocation energy per unit area of the interface can be estimated to be $\gamma \simeq \varepsilon/l_d$, where γ can be treated as an 'interfacial tension', for the director lying parallel to the interface. In our treatment, the free energies of the TGB_C structure predicted by Renn and Lubensky and that found by the Bordeaux group are the same.

In the case of the $UTGB_{C*}$ phase the interface develops undulations along two mutually orthogonal directions. This can be expected to cost additional interfacial energy. If the TGB helix axis is taken to be along the Z-axis, the undulation can be described by a height function $h(x, y)$. The simplest form of h which gives a two-dimensional modulation of period $2\pi/q_u$ is

$$h(x, y) = A \cos(q_u x) + A \cos(q_u y). \tag{1}$$

The interfacial energy per unit projected area on the XY-plane is given by

$$f_{int} \simeq \gamma[1 + (\nabla_x h)^2 + (\nabla_y h)^2]^{1/2}. \tag{2}$$

As already described, the director prefers to be parallel to the interface. Any deviation from this preferred orientation costs energy. This is analogous to the anisotropic interfacial tension at a SmC*–isotropic interface [23, 27]. This anisotropic energy cost can be expressed as

$$f_{aniso} = \tilde{\gamma}(\mathbf{n} \cdot \mathbf{l})^2 \tag{3}$$

where $\mathbf{n}$ is the Frank-director, $\mathbf{l}$ is the unit normal to the interface and $\tilde{\gamma} > 0$. For small amplitude undulations

$$\mathbf{l} \simeq \frac{(-\nabla_x h, -\nabla_y h, 1)}{[1 + (\nabla_x h)^2 + (\nabla_y h)^2]^{1/2}}. \tag{4}$$

Introducing interfaces is favourable when the chiral energy gained due to the twist across the interface exceeds the positive contribution given by $f_{int} + f_{aniso}$. In the TGB_A phase, the average rate of twist is given by

$$\langle q_{tgb} \rangle = \langle (\mathbf{n} \cdot \nabla \times \mathbf{n}) \rangle \simeq \frac{\Delta\beta}{l_b} \tag{5}$$

where $\Delta\beta$ is the angle between the smectic layer normals of any two adjacent blocks. This twist across each interface gives an average gain in the chiral energy per unit volume [3]

$$f_{twist} = -\Lambda \langle q_{tgb} \rangle = -\Lambda \frac{\Delta\beta}{l_b} \tag{6}$$

where Λ is the chiral strength.

It is known from experimental studies [28, 15] that as the temperature is reduced, the pitch increases in the cholesteric and the TGB phases. This increase is quite sharp in the TGB_C and the $UTGB_{C*}$ phases. However,

for the sake of simplicity, we assume that $\Delta\beta$ and l_b (and hence the TGB pitch) remain constant, independent of temperature in all the TGB phases. Thus, we assume that equation (6) for the twist energy holds even in the $UTGB_{C*}$ phase.

We are mainly interested in the various phases that can occur below the TGB_A phase when the local smectic ordering within the layers changes from SmA-like to SmC-like. Below a certain temperature T_{AC}, the smectic layers develop tilt order. The TGB blocks can then be either SmC-like (unwound SmC*) or SmC*-like. We adopt a simple Landau theory for the SmA–SmC* transition [29, 25], instead of the detailed Chen–Lubensky theory [30].

In the TGB phases, let the TGB helix axis be along the Z-axis. To describe the structure within a given block, we choose a local co-ordinate system (X', Y', Z') which is rotated about the Z-axis such that the X'-axis makes an angle β with respect to the space-fixed X-axis. Thus, in the TGB_A and the $UTGB_{C*}$ phases, β is the angle between the smectic layer normal of that block and the X-axis. In the TGB_C phase, β is the angle between the projection of the layer normal of that block on the XY-plane and the X-axis. The components of the Frank-director in a given block are then given by $n_{x'} = \cos\theta$, $n_{y'} = \sin\theta\cos\phi$, $n_{z'} = \sin\theta\sin\phi$, where θ is the tilt angle and ϕ is the angle the **c**-vector, which is the projection of the Frank-director on the plane of the layers' ($Y'Z'$-plane), makes with respect to the Y'-axis.

In the TGB_C phase, the **c**-field is assumed to be uniform within any given block. In the $UTGB_{C*}$ phase, however, the **c**-vector precesses along the layer normal in each block. Assuming θ to be small, the free energy density of the TGB blocks can be written in the form [29, 25]

$$f_{block} = \frac{a}{2}\theta^2 + \frac{b}{4}\theta^4 + \frac{K_c}{2}\theta^2(\nabla'\phi)^2 + \Lambda\theta^2\frac{\partial\phi}{\partial x'} - \frac{K_b^*}{2}\theta\left(\sin\phi\frac{\partial\phi}{\partial y'} + \cos\phi\frac{\partial\phi}{\partial z'}\right) - K_{bt}\theta^3\left(\sin\phi\frac{\partial\phi}{\partial y'} + \cos\phi\frac{\partial\phi}{\partial z'}\right)\frac{\partial\phi}{\partial x'} \qquad (7)$$

where $a = \alpha(T - T_{AC})$. K_c is the elastic constant corresponding to twist deformations in the **c**-field. A pure twist deformation in the **c**-field involves both twist and bend in the Frank-director-field. The term with the coefficient K_c is obtained by using the usual one elastic constant approximation in the Frank free energy expression. The term with the coefficient Λ is responsible for the spontaneous twist of the **c**-vector in the SmC* phase. The term with the coefficient K_b^* is allowed by symmetry since the medium is chiral. Physically, this term arises because an in-plane bend in the **c**-field produces a twist in the **n**-field and hence there can be a gain in chiral energy for a particular sign of bend. The last term describes a cross-coupling between the twist- and bend-deformations in the **c**-field of neighbouring layers. It should be mentioned that in writing the above expression we have ignored all polarization effects. This is because in the harmonic approximation the polarization-dependent terms merely renormalize some of the coefficients in equation (7).

As already explained, any deviation of the director from the local tangent plane of the interface costs additional energy f_{aniso}. If the director has to be parallel to the interface, the condition $(\mathbf{n}\ \mathbf{l}) = 0$ should be satisfied. For small amplitude modulations, with the height function (1) transformed to the block fixed frame, this condition for a block with $\beta = 0$ becomes

$$Aq_u\sin(q_u x') + Aq_u\tan\theta\cos\phi\sin(q_u y') + \tan\theta\sin\phi = 0. \qquad (8)$$

The above equation has no analytical solution and numerically we could not find a solution which gives a continuous spatial variation of ϕ. Therefore, we look for director profiles which (i) give a *smooth* variation of $\phi(x', y')$ within a block and (ii) lower the value of $\langle(\mathbf{n}\ \mathbf{l})^2\rangle$ compared with that for a perfect SmC* structure within the block. We find that the following ansatz for the ϕ-distribution in a block with $\beta = 0$ satisfies the above criteria:

$$\phi(\beta = 0) = -q_u x' - \tan^{-1}[\tan\theta\sin(q_u y')]. \qquad (9)$$

This generates a continuous variation of ϕ along the local smectic layer normal, which is parallel to the X'-axis and a periodic distortion within the layers along the Y'-axis.

The description of the block structure clearly depends on β. The undulation already fixes a square lattice with a periodicity $2\pi/q_u$. We note that if $\tan\beta$ is an irrational number, it is not possible to define a 2D unit cell over which the structure (undulation and the $\phi(x', y')$-profile) repeats itself and hence to evaluate the average energy per unit area. The geometrical aspects of problems of this type have been discussed in great detail in relation to 2D incommensurate structures and quasicrystals [31]. This interesting problem is very complicated and we shall not persue it in this paper.

We simplify the problem drastically by assuming that in *all* the TGB phases β can take only values given by $m\pi/4$, where m labels the block number. It is then clear that the unit cell of the square lattice given by the undulations is adequate for calculating the average energy referred to above. Further, along the TGB helix axis (Z-axis), we have to average only over two blocks,

one with $\beta = 0$ and the other with $\beta = \pi/4$, as all other blocks are related by symmetry to these two. The square grid structure of the $UTGB_{C*}$ phase is also consistent with the even more drastic assumption that the twist angle between successive blocks, $\Delta\beta = \pi/2$. This can lower f_{aniso} compared with a structure with $\Delta\beta = \pi/4$. Indeed, Levelut *et al.* [32] have recently proposed that in the smectic Q phase exhibited by some highly chiral compounds with an underlying antiferroelectric structure, $\Delta\beta$ can be $\pi/2$ or even $2\pi/3$. As discussed by these authors, such structures have an extremely short pitch (~ 100 Å) and they are described in terms of Scherk's first surface as in the case of some diblock copolymers [33]. On the other hand, the measured values of the TGB pitch in the $UTGB_{C*}$ phase is $\sim 1\,\mu m$ and we think that $\Delta\beta = \pi/2$ is unlikely. In any case, with any set of fixed values of $\Delta\beta$ and l_b, the qualitative features of the phase diagrams are unlikely to change.

In analogy with equation (9), the director configuration in a block with $\beta = m\pi/4$ is now assumed to be

$$\phi(x', y') = -q'x' - \tan^{-1}[\tan\theta \sin(q'y')] \qquad (10)$$

where $q'(\beta = m\pi/4) = q_u/(\sin\beta + \cos\beta)$.

In writing the above ansatz we have assumed that within the blocks ϕ is constant along Z', which is the TGB twist-axis direction, since most of the twist distortion is confined to the grain boundary region. In the TGB_A and TGB_C phases, ϕ is constant along X' and Y' also. But in the $UTGB_{C*}$ phase, ϕ varies continuously along X' and oscillates along Y'. With the ϕ-profile given by equation (10), the contribution from the last two terms in equation (7) with coefficients K_b^* and K_{bt}, integrated over a unit cell of the square lattice, vanishes. Therefore, the free energy density of the blocks can be written in the form

$$f_{block} = \frac{a}{2}\theta^2 + \frac{b}{4}\theta^4 + \frac{K_c}{2}\theta^2\left[\left(\frac{\partial\phi}{\partial x'}\right)^2 + \left(\frac{\partial\phi}{\partial y'}\right)^2\right] + \Lambda\theta^2\frac{\partial\phi}{\partial x'}. \qquad (11)$$

In the cholesteric phase, the equilibrium wave number obtained by minimizing the Frank free energy expression is $q_o = -\Lambda/K$, where K is the twist elastic constant. In practice, the pitch of the cholesteric increases as the temperature is lowered. The pitch in the TGB_A phase can be expected to be larger compared with that in the cholesteric phase. Experimentally the pitch increases continuously on going from the cholesteric to the TGB_A phase [15, 28]. In our calculations we neglect the temperature dependence of the pitch in the TGB phases and assume $\langle q_{tgb}\rangle = q_o/2 = -\Lambda/2K$ in all the TGB phases. Since $\Delta\beta = \pi/4$, there are eight blocks in a TGB pitch. Thus, $l_b = \pi/4|\langle q_{tgb}\rangle| = \pi K/4\Lambda$.

The various TGB phases and the SmC* phase can be described as

$$TGB_A: \theta = 0, \quad l_b = \pi/4|\langle q_{tgb}\rangle|, \quad q_u = 0;$$
$$TGB_C: \theta \neq 0, \quad \phi = const., \quad l_b = \pi/4|\langle q_{tgb}\rangle|, \quad q_u = 0;$$
$$UTGB_{C*}: \theta \neq 0, \quad \phi \equiv \phi(x', y'), \quad l_b = \pi/4|\langle q_{tgb}\rangle|, \quad q_u \neq 0;$$
$$SmC*: \theta \neq 0, \quad \phi = q_c x', \quad l_b = \infty;$$

where q_u corresponds to the periodicity of the two-dimensional modulation of the interface as described by equation (1) and $q_c = -\Lambda/K_c$ to that of the equilibrium SmC* pitch obtained from the free energy density equation (11).

In the SmC* phase, the free energy density given by equation (11) reduces to

$$f_{C*} = \frac{a}{2}\theta^2 + \frac{b}{4}\theta^4 - \frac{\Lambda^2}{2K_c}\theta^2. \qquad (12)$$

In the TGB_A phase, the average energy per unit volume, which is just the sum of the average interfacial energy f_{int}, and the twist energy, f_{twist}, is

$$f_{TGB_A} = \frac{\gamma}{l_b} - \frac{\Lambda\Delta\beta}{l_b} \qquad (13)$$

where $\Delta\beta$ is assumed to be $\pi/4$ as in the $UTGB_{C*}$ phase. There is no contribution to f_{TGB_A} from f_{block}, since $\theta = 0$. In the Renn–Lubensky model, the TGB_A phase is unstable with respect to the SmA phase as the temperature is lowered. This is because the dislocation energy which depends on the smectic layer compression modulus increases with reduction in temperature. This factor also contributes to the TGB_C–SmC* transition in their model [3, 10]. In our model this is equivalent to an increase in γ. As we have ignored the temperature dependence of γ, we do not get TGB_A–SmA or $TGBA_A$–SmC* transitions.

In the TGB_C phase ϕ is constant in a given block and the only contributions to the free energy density from the smectic blocks are from the first two terms in equation (11), which are independent of ϕ. The interfacial part is the same as that for the TGB_A. Thus, the average free energy density of the TGB_C phase is

$$f_{TGB_C} = f_{TGB_A} + \frac{a}{2}\theta^2 + \frac{b}{4}\theta^4. \qquad (14)$$

Unlike in the TGB_A and TGB_C phases, the block energy in the $UTGB_{C*}$ phase depends on the orientation of the smectic layer normal with respect to the undulation wave vectors. Therefore, the total free energy density has to be averaged over a three-dimensional unit cell. The unit cell is defined by the lattice spacing of the interface modulation $a = 2\pi/q_u$ and the TGB pitch $p_{tgb} = \pi/\langle q_{tgb}\rangle$.

Using equations (2), (3), (6) and (11) for f_{int}, f_{aniso}, f_{twist} and f_{block}, respectively, the averaged total free energy per unit volume is

$$f_{UTGB_{C*}} = \frac{1}{N}\sum_{m=1}^{N}\left[\frac{q'^2}{4\pi^2}\int_0^{2\pi/q'}dx'\int_0^{2\pi/q'}dy' \times\left\{f_{block}+f_{twist}+\frac{f_{int}}{l_b}+\frac{f_{aniso}}{l_b}\right\}_m\right] \quad (15)$$

where N denotes the number of blocks within a TGB pitch. We minimize the averaged energy density $f_{UTGB_{C*}}$ with respect to the undulation amplitude A and the wave vector magnitude q_u. We use the Gaussian Quadrature method [34] for performing the integration and the Simplex method [34] for the minimization.

We fix the constants α and b such that the temperature variation of θ, where $\theta^2 = \alpha(T^*_{AC} - T)/b$ for $T < T^*_{AC}$, and $T^*_{AC} = T_{AC} - \Lambda^2/\alpha K_c$ [25] agrees reasonably well with the experimental data. We choose a value for K which is typical of the cholesteric phase. For simplicity, we take $K_c = K$. A rough estimate of the grain boundary energy per unit area for the TGB_A phase near the lower critical chiral strength Λ_o is given by $\gamma \simeq \varepsilon/l_d = \Lambda_o d/l_d$, where ε is the energy per unit length of the screw dislocations [3]. With the values (in cgs units) $\Lambda_{cl} = 0.04$, $d = 30 \times 10^{-8}$ and $l_d = 100 \times 10^{-8}$ we get $\gamma = 1.2 \times 10^{-2}$. Note that this is of the same order of magnitude as the interfacial tension estimated for the smectic–isotropic interface ($\sim 10^{-2}$ dyn cm^{-1}) [23]. The anisotropic part of the interfacial tension for the smectic–isotropic interface is typically about 1.5 times larger [23].

Based on the above considerations, we choose the following parameters for the calculations (in cgs units): $\alpha = 0.1 \times 10^8$ and $b = 50.0 \times 10^8$, $K_c = K = 0.2 \times 10^{-6}$, $\gamma = 3.0 \times 10^{-2}$ and $T_{AC} = 63.0$°C. We calculate the average free energy density as a function of temperature in the various phases for different values of the chiral strength Λ and the anisotropy in the interfacial tension $\tilde{\gamma}$. The results of these calculations are discussed below.

3. Results and discussion

Figure 4 shows the phase diagram obtained as a function of $\tilde{\gamma}$, which is the anisotropic part of the interfacial tension. The temperature vs. chiral strength phase diagram is shown in figure 5. The variations in the lattice spacing and amplitude of the square modulation as functions of temperature for specific values of Λ and $\tilde{\gamma}$ are shown in figures 6 and 7 respectively.

We are interested in understanding the relative stability of the various phases that can occur below the TGB_A phase. Therefore, we always start with a TGB_A phase with $T > T^*_{AC}$ and chiral strength $\Lambda = \sqrt{K\gamma}$, which is obtained using equation (13). Below T^*_{AC}, the tilt angle θ becomes non-zero and increases with reduction

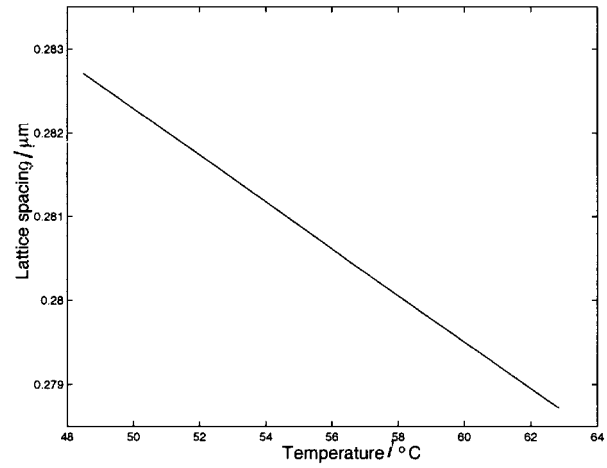

Figure 6. Temperature dependence of the lattice spacing ($2\pi/q_u$) of the square grid, obtained by minimizing equation (15) with respect to A and q_u for $\Lambda = 0.0396$. Experiments show that the lattice spacing drops sharply just below the TGB_A–$UTGB_{C*}$ transition temperature and then remains more or less constant throughout the $UTGB_{C*}$ range on lowering the temperature [15].

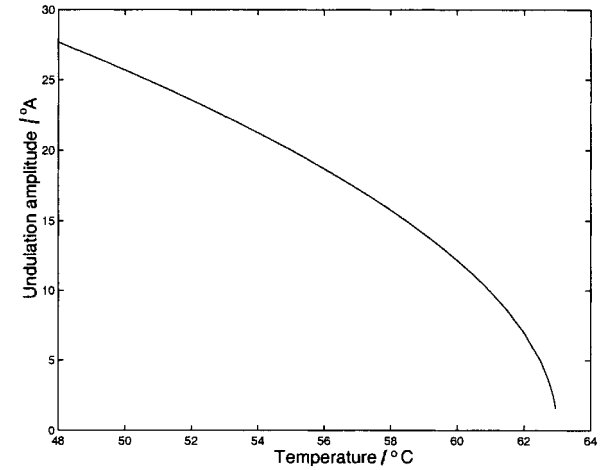

Figure 7. Temperature dependence of the amplitude A of the height modulation for $\Lambda = 0.0396$. Note that A behaves like an order parameter for the $UTGB_{C*}$ phase.

in temperature as $\theta^2 \simeq \alpha(T^*_{AC} - T)/b$. This increase in the tilt angle at constant $\tilde{\gamma}$ and Λ has the following consequences in the $UTGB_{C*}$ phase. (i) Both the chiral energy gain and the elastic energy cost from f_{block} given by equation (11) increase as θ^2; the net gain in the bulk is lower than that in the SmC* phase since the $\phi(x', y')$ profile described by equation (10) differs from that for the SmC* phase. (ii) f_{int} increases as the amplitude A of the height modulation increases (figure 7). (iii) f_{aniso} increases as the mismatch at the interface grows with θ.

First, let us consider the phase diagram constructed as a function of $\tilde{\gamma}$ for a fixed chiral strength Λ (figure 4). For large values of $\tilde{\gamma}$, the TGB_C phase is preferred

over the $UTGB_{C*}$ phase mainly because the former has $f_{aniso} = 0$. As the temperature is lowered the tilt angle increases and at some stage the chiral energy gained in the SmC* phase exceeds that from $f_{twist} + f_{int}$ in the TGB_C phase. Since $f_{aniso} = 0$, this transition is independent of $\tilde{\gamma}$. As $\tilde{\gamma}$ is reduced, the additional interfacial energy cost from $f_{int} + f_{aniso}$ in the $UTGB_{C*}$ phase becomes small compared with the chiral energy gained in the blocks with $\phi(x', y')$ given by equation (10). Thus the $UTGB_{C*}$ phase is favoured over the TGB_C phase. But, as θ increases with decrease in temperature, $f_{int} + f_{aniso}$ also increases. Further, the energy cost from the $\phi(x', y')$ distortions reduces the net gain from f_{block}. These factors cause the $UTGB_{C*}$–SmC* transition. There is also a narrow range of $\tilde{\gamma}$ in which there is a transition from $UTGB_{C*}$ to TGB_C.

Next, we consider the stability regions of the various phases for a fixed value of the anisotropic part of the interfacial tension $\tilde{\gamma}$ (figure 5):

Moderate chiral strength. When the chiral strength is increased beyond a critical value Λ_o, the gain in chiral energy overcomes the energy cost from the interface. Above T^*_{AC}, the TGB_A structure is favoured. Below T^*_{AC}, for small tilt angles, the chiral energy gained in the bulk by having a helical structure (equation 10) is not very significant compared with the energy gained across a flat interface with $f_{aniso} = 0$. This makes the TGB_C structure more favourable compared with that of SmC*. As the temperature is lowered, the chiral energy gained by letting the director precess along the smectic layer normal increases as θ^2. Below a certain temperature the bulk energy gain in the SmC* phase exceeds that from $f_{twist} + f_{int}$ in the TGB_C phase. The $UTGB_{C*}$ phase is not favoured because f_{int}, f_{aniso} and elastic energy from f_{block} also increase with tilt angle. Hence there is a direct transition from the TGB_C to the SmC* phase.

Large chiral strength. Interfaces are strongly favoured for large values of Λ. The energy gained in the bulk by having $UTGB_{C*}$ blocks becomes considerable even for small tilt angles. But the gain in the bulk free energy from the helical structure within the blocks *alone* is less than that from an undistorted SmC* structure. Nevertheless, the $UTGB_{C*}$ phase is favoured because the gain in energy from $f_{twist} + f_{block}$ is large enough compared with the energy cost $f_{int} + f_{aniso}$. As the temperature is lowered, $f_{int} + f_{aniso}$ increases. Also, the difference between the bulk energies of $UTGB_{C*}$ blocks and the SmC* phase becomes larger. For these two reasons, there is a transition from the $UTGB_{C*}$ to the SmC* phase below a certain temperature. As Λ increases, the $UTGB_{C*}$–SmC* transition occurs at lower temperatures.

As in the case of the cholesteric to blue phase transition [1], where a one-dimensionally modulated structure transforms to a three-dimensionally modulated one, the transition from TGB_A to $UTGB_{C*}$ and $UTGB_{C*}$ to SmC* can be weakly first order. In the context of our highly simplified model we have not explored such details of the various transitions.

There have been some reports of observing a TGB_{C*} liquid crystal with a hexagonal rather than a square lattice [17, 35]. In the framework of the model presented above, it is easy to visualize a structure with three undulatory waves whose wave vectors are at a mutual angle of $2\pi/3$ radians. A detailed calculation of the relative stability of the resulting hexagonal and square lattices is in progress.

4. Conclusion

We have carried out a simple analysis of the stabilities of the various TGB phases. In our model, the grain boundaries are treated as uniform interfaces. The blocks and the grain boundaries in the $UTGB_{C*}$ phase are modelled using an ansatz based on experimental observations. Although many details of the structure of the blocks and the grain boundaries are not included, this highly simplified model is able to account for the relative stabilities of the various TGB phases. For a detailed comparison with experiments the temperature dependences of the various parameters must be taken into account. The values of γ and $\tilde{\gamma}$ as well as the elastic constants can be expected to increase as the temperature is reduced. This can, in principle, lead to the experimentally observed increase in the TGB pitch with lowering of temperature. In our analysis, we have ignored the temperature dependence of these parameters. Nevertheless, we believe that this simple model captures the physical mechanisms responsible for the formation of these complex structures.

References

[1] De Gennes, P. G., and Prost, J., 1993, *The Physics of Liquid Crystals*, 2nd Edn (Oxford Science Publications).
[2] De Gennes, P. G., 1972, *Solid State Commun.*, **10,** 753.
[3] Renn, S. R., and Lubensky, T. C., 1988, *Phys. Rev. A*, **38,** 2132.
[4] Chaikin, P. M., and Lubensky, T. C., 1995, *Principles of Condensed Matter Physics* (Cambridge University Press).
[5] Abrikosov, A. A., 1957, *Zh. eksp. teor. Fiz.*, **32,** 1442.
[6] Abrikosov, A. A., 1957, *Sov. Phys. JETP.*, **5,** 1174.
[7] Goodby, J. W., Waugh, M. A., Stein, S. M., Chin, E., Pindak, R., and Patel, J. S., 1989, *Nature*, **337,** 449.
[8] Ihn, K. J., Zasadzinski, J. A. N., Pindak, R., Slaney, A. J., and Goodby, J. W., 1992, *Science*, **258,** 275.
[9] Benguigui, L., 1998, *Liq. Cryst.*, **25,** 505.
[10] Renn, S. R., and Lubensky, T. C., 1991, *Mol. Cryst. liq. Cryst.*, **209,** 349.

[11] Navailles, L., Pindak, R., Barois, P., and Nguyen, H. T., 1995, *Phys. Rev. Lett.*, **74,** 5224.
[12] Dozov, I., 1995, *Phys. Rev. Lett.*, **74,** 4245.
[13] Hatwalne, Y., and Lubensky, T. C., unpublished results.
[14] Renn, S. R., 1992, *Phys. Rev. A*, **45,** 953.
[15] Pramod, P. A., Pratibha, R., and Madhusudana, N. V., 1997, *Curr. Sci.*, **73,** 761.
[16] Pramod, P. A., Pratibha, R., Sobha, R. W., and Madhusudana, N. V., *Ferroelectrics.* (in the press).
[17] Kuczynski, W., and Stegemeyer, H., 1998, *Proc. SPIE*, **3318,** 90.
[18] Goodby, J. W., 1999, in *Structure and Bonding*, edited by D. M. P. Mingos (Springer-Verlag).
[19] Sadashiva, B. K., 1999, *Pramana.*, **53,** 213.
[20] Riberiro, A. C., Barois, Ph., Galerne, Y., Oswald, L., and Guillon, D., 1999, *Eur. J. Phys.*, **B11,** 121.
[21] Srajer, G., Pindak, R., Waugh, M. A., Goodby, J. W., and Patel, J. S., 1990, *Phys. Rev. Lett.*, **64,** 1545.
[22] Fournier, J. B., and Durand, G., 1991, *J. Phys. II (Fr).*, **1,** 845.
[23] Fournier, J. B., Dozov, I., and Durand, G., 1990, *Phys. Rev. A*, **41,** 2252.
[24] Navailles, L., Pansu, B., Giorre-Talini, L., and Nguyen, H. T., 1998, *Phys. Rev. Lett.*, **81,** 4168.
[25] Goodby, J. W., Blinc, R., Clark, N. A., Lagerwall, S. T., Osipov, M. A., Pikin, S. A., Sakurai, T., Yoshino, K., and Zeks, B., 1991, *Ferroelectric Liquid Crystals* (Gordon and Breach).
[26] Hatwalne, Y., and Madhusudana, N. V., unpublished results.
[27] Galatola, P., Fournier, J. B., and Durand, G., 1994, *Phys. Rev. Lett.*, **73,** 2212.
[28] Isaert, N., Navailles, L., Barois, P., and Nguyen, H. T., 1994, *J. Phys. II (Fr).*, **4,** 1501.
[29] Pikin, S. A., and Indenbom, V. L., *Usp. Fiz. Nauk.*, 1978, **125,** 251; [*Sov. Phys.—Usp.*, **21,** 487 (1979)].
[30] Chen, J., and Lubensky, T. C., 1976, *Phys. Rev. A*, **14,** 1202.
[31] See, e.g., 1987, *The Physics of Quasicrystals*, edited by P. J. Steinhardt and S. Ostlund (World Scientific).
[32] Levelut, A. M., Hallouin, E., Bennemann, D., Heppke, G., and Lotzsch, D., 1997, *J. Phys. II (Fr).*, **7,** 981.
[33] Gido, S. P., and Thomas, E. L., 1997, *Macromolecules*, **30,** 3739.
[34] Press, W. H., Flannery, B. P., Teukolsky, S. A., and Vetterling, W. T., 1982, *Numerical Recipes*, 2nd Edn (Cambridge University Press).
[35] Galerne, Y., Private communication.